Simulation and Design of Applied Electromagnetic Systems
T. Honma (Editor)

The optimum configurations of SQUID sensors for the magnetocardiogram and magnetoencephalogram

H. Saotome and Y. Saito

College of Engineering, Hosei University, 3-7-2 Kajino, Koganei, Tokyo 184, Japan

Abstract

This paper deals with optimum SQUID sensor configurations for biological system applications. It is shown that the optimum SQUID sensor configurations make it possible to establish locally orthogonal coordinate systems at the measurement surfaces. This leads to a faster field source searching algorithm based on the sampled pattern matching method. Some test examples demonstrate that current distribution in the heart can be estimated at a speed of about ten times faster than the conventional sampled pattern matching algorithm.

1. INTRODUCTION

Obtaining the current signal distribution in a human body from electromagnetic field data measured over the body takes a very important role in medical diagnosis. This process is reduced to solving the inverse problem. In order to identify the current signal distributions in the human heart from a magnetocardiogram (MCG) and in the human brain from a magnetoencephalogram (MEG), we have successfully developed the sampled pattern matching (SPM) algorithm [1-5]. Moreover, this algorithm has been applied to non-destructive testing [6].

In the previous studies, the Cartesian coordinate system was used to estimate current element (or dipole) vectors. In this paper, we propose the locally orthogonal coordinate systems, such as the cylindrical and spherical coordinate systems, for MCG and MEG analyses, respectively. With the result of employing the locally orthogonal coordinate systems, we reveal that the optimum SQUID sensor configurations make it possible to implement the SPM method for fast medical diagnosis with MCGs and MEGs.

2. FASTER SPM METHOD UTILIZING THE LOCALLY ORTHOGONAL COORDINATE SYSTEMS

The MCG and MEG analyses can be reduced to searching for distribution of the source current density J. This problem is expressed by the following integral equation:

$$\mathbf{H} = \nabla \times \int_{U} G\, \mathbf{J}\, dv, \tag{1}$$

where H is the magnetic field intensity and G denotes the Green function. In (1), the product J dv corresponds to the current dipole vector. The measured magnetic field pattern (MCG or MEG) is caused by current dipole vectors. Therefore, the identification of current distribution is carried out by estimating not only current dipole positions but also their directions. Identifying the current dipole direction requires considerable CPU time in the Cartesian coordinate system. For example, 72-time SPM processes are necessary at the same spatial position when the angular resolution is 5 degrees [3-5]. The locally orthogonal coordinate systems, i.e. the cylindrical and spherical coordinate systems proposed in this paper, can remove the angular subdivision, so that an efficient SPM implementaion can be carried out. This is because the magnetic field pattern on the measurement surface

of these coordinate systems can be decomposed into two orthogonal field pattern components whereas it can not be done in the Cartesian coordinate system.

With these locally orthogonal coordinate systems, the system equation for the MCG and MEG analyses is derived from (1). By discretizing a target volume into m small subdivisions, we get

$$\mathbf{u} = \sum_{j=1}^{m} (\alpha_{pj}\, \mathbf{d}_{pj} + \alpha_{qj}\, \mathbf{d}_{qj}); \quad p=r,\ q=\theta \quad \text{or} \quad p=\theta,\ q=\phi; \tag{2}$$

where $\mathbf{u}$ shows a MCG or MEG pattern, α_{pj} and α_{qj} are p and q components of a current dipole vector at a position j. When we have n measurement points, the n-dimensional vectors $\mathbf{d}_{pj}$ and $\mathbf{d}_{qj}$ show the estimated magnetic field patterns due to α_{pj} and α_{qj}, respectively. In the proposed coordinate systems, the orthogonality between $\mathbf{d}_{pj}$ and $\mathbf{d}_{qj}$

$$\mathbf{d}_{pj}^{T} \cdot \mathbf{d}_{qj} = 0, \tag{3}$$

is satisfied as shown in Fig. 1 for the cylindrical coordinates and Fig. 2 for the spherical coordinates. Making the most of (3), the pattern matching rates of $\mathbf{d}_{pj}$ and $\mathbf{d}_{qj}$ with respect to the measured MCG or MEG $\mathbf{u}$ can be independently evaluated by

$$\gamma_{tj} = \mathbf{u}^{T} \cdot \mathbf{d}_{tj} \,/\, (\|\mathbf{u}\|\, \|\mathbf{d}_{tj}\|); \quad t=p,\ q. \tag{4}$$

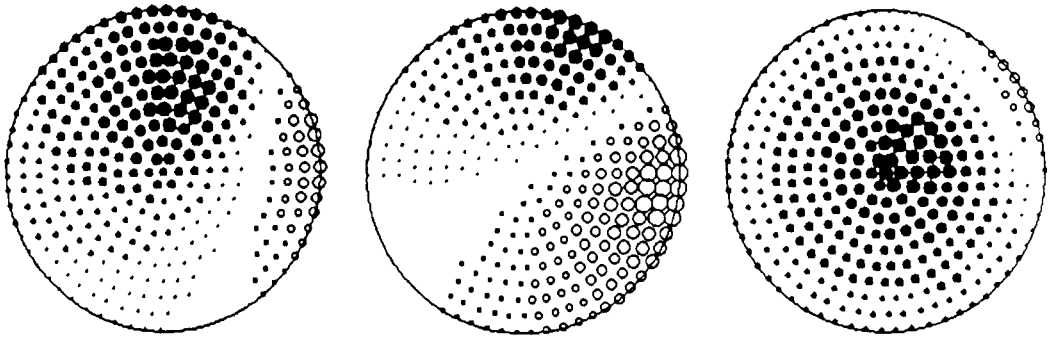

(a) $\mathbf{u}$ pattern (b) $\mathbf{d}_r$ pattern (c) $\mathbf{d}_\theta$ pattern

Figure 1. Magnetic field patterns normal to a circular measurement surface of the radius r=1 in the cylindrical coordinate system when the current dipole vector $(\alpha_r, \alpha_\theta)=(1, 1)$ is located at $(r, \theta, z)=(0.8, \pi/6, 0.8)$. The circles ● and ○ indicate N and S poles, respectively. Obviously, $\mathbf{u}=\mathbf{d}_r+\mathbf{d}_\theta$ and $\mathbf{d}_r^{T} \cdot \mathbf{d}_\theta=0$ are held.

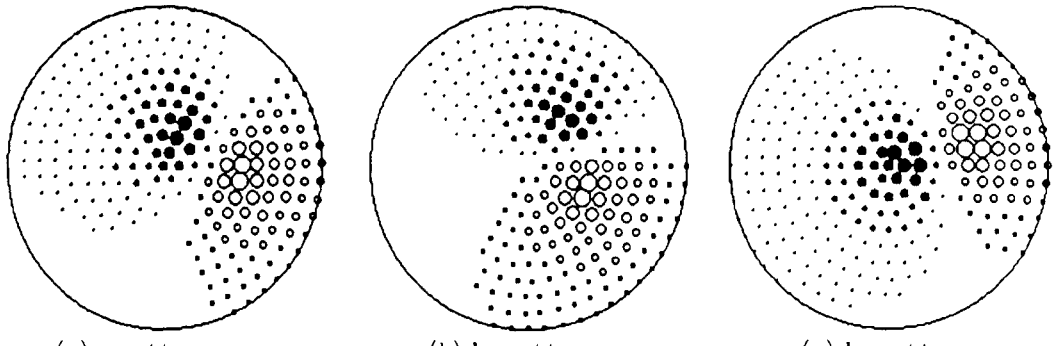

(a) $\mathbf{u}$ pattern (b) $\mathbf{d}_\theta$ pattern (c) $\mathbf{d}_\phi$ pattern

Figure 2. Magnetic field patterns normal to a spherical measurement surface of the radius r=1 and the angle $\theta \leq \pi/4$ in the spherical coordinate system when the current dipole vector $(\alpha_\theta, \alpha_\phi)=(1, 1)$ is located at $(r, \theta, \phi)=(0.8, \pi/12, \pi/12)$. The circles ● and ○ indicate N and S poles, respectively. $\mathbf{u}=\mathbf{d}_\theta+\mathbf{d}_\phi$ and $\mathbf{d}_\theta^{T} \cdot \mathbf{d}_\phi=0$ are held.

From (4), it is possible to obtain the amplitude of the normalized current dipole spectrum [3,4], γ_j, and its spatial angle on the p-q plane, ψ_j:

$$\gamma_j = \sqrt{\gamma_{pj}^2 + \gamma_{qj}^2}, \tag{5}$$

$$\psi_j = \tan^{-1}(\gamma_{qj} / \gamma_{pj}), \tag{6}$$

where ψ_j is determined by taking account of the signs of γ_{pj} and γ_{qj}. After finding out the first current dipole vector, we continue with the procedures similar to (4)-(6) up to the peak of γ [1-6].

Therefore, employing the proposed coordinate systems for the MCG and MEG analyses removes the repetitive process for determining the angle of a current dipole vector. As a result, we suggest the optimum configurations of SQUID sensors as shown in Figs. 1 and 2, rather than mounting them in a square or rectangular grid.

3. EXAMPLES

Figure 3 shows the normalized current dipole vector spectrum distributions obtained from three MCGs of reference [7]. From the comparison of the results obtained by the conventional and proposed algorithms, it is revealed that the

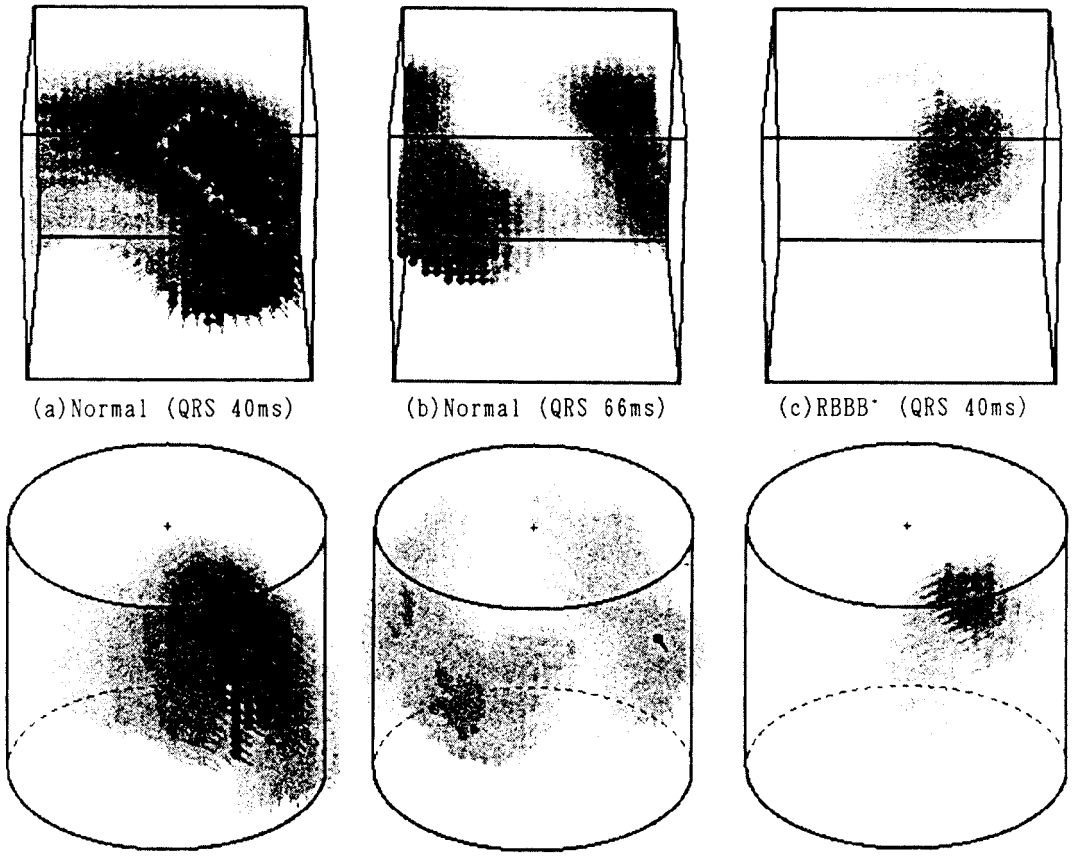

Figure 3. Comparison of the estimated current dipole vector spectrums (γ>0.8) obtained by the conventional and proposed algorithms. (a)-(c)Obtained by the conventional algorithm with the Cartesian coordinate system; m=13225, n=36, $\Delta\psi$=5[deg]. (d)-(f)Obtained by the proposed algorithm with the cylindrical coordinate system; m=14150, n=32. *Right Bundle Branch Block syndrome.

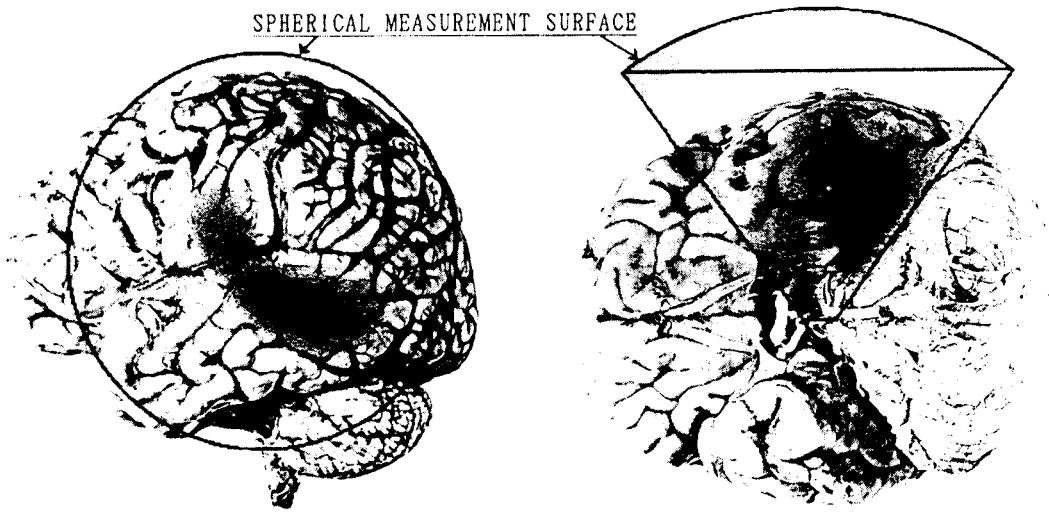

(a)Profile (b)Bottom view

Figure 4. Current dipole vector spectrum distribution (γ>0.9) obtained by applying our new algorithm to the MEG at 110ms after hearing the voice of "ah": m=75221, n=37. The target region is enclosed by solid lines.

proposed method provides the comparable results to the conventional ones even if the angular subdivision for current dipole vectors has not been carried out. The results of Figs. 3(d)-(f) were obtained more than ten times faster compared with those of Figs. 3(a)-(c).

Using a 37-channel SQUID of which the sensors are mounted on a spherical surface having the radius of curvature, 122mm, Prof.Kuriki's group in Hokkaido University measured a MEG when a person heard a voice of "ah" [8]. The application of our new method to the MEG at 110ms after hearing the voice provided the current dipole distribution in his/her brain as shown in Fig. 4.

4. CONCLUSION

We have proposed the locally orthogonal coordinate systems for the MCG and MEG diagnoses based on the SPM method, as well as the optimum SQUID sensor configurations. Thus, our novel algorithm proposed in this paper can provide medical doctors with current distributions in the heart and in the brain faster than the conventional method.

5. REFERENCES

1 Y.Saito, et al., J. Appl. Phys., 67, No.9, (1990), pp.5830-5832.
2 H.Saotome, et al., Trans. IEE, Japan, Vol.112-A, No.4, (1992), pp.279-286.
3 H.Saotome, et al., Trans. IEE, Japan, Vol.113-C, No.1, (1993), pp.101-108.
4 H.Saotome, et al., Electromagnetic Field Source Searching from the Local Field Measurement, Int. J. Appl. Electromag. Matrls, (1993), in Press.
5 H.Saotome, et al., A Neural Behavior Estimation by the Generalized Correlative Analysis, IEEE Trans. Magn., March, (1993), in Press.
6 H.Saotome, et al., Crack Identification in Metallic Materials, IEEE Trans. Magn., March, (1993), in Press.
7 K.Watanabe, et al., (K.Atsumi et al., Ed., Biomagnetism' 87, Tokyo Denki University Press, Japan, 1988), pp.346-349.
8 S.Kuriki, et al., J. Japan Biomag. Bioelectromag. Society, Vol.5, No.1, June (1992), pp.20-23.